



SIMULATION OF SEISMIC AMBIENT NOISE: I. RESULTS OF H/V AND ARRAY TECHNIQUES ON CANONICAL MODELS

**Sylvette BONNEFOY-CLAUDET¹, Cécile CORNOU², Jozef KRISTEK³, Matthias
OHRNBERGER⁴, Marc WATHELET⁵, Pierre-Yves BARD¹, Peter MOCZO³, Donat FAEH²,
Fabrice COTTON¹**

SUMMARY

Numerical simulation of noise in well-controlled 1D and 3D structures is used to investigate the possibilities and limits of the H/V and the array techniques to retrieve the right information on site characteristics (fundamental frequency, velocity profile). The robustness of the H/V and array techniques in providing the fundamental frequency and the S-wave velocity profile of horizontally layered structures is shown in this study. The limits of these methods are highlighted in case of dipping layers, for which the H/V peak frequency exhibits a significant deviation from the theoretical 1D local value, while the velocity profile obtained by array analysis is related to average thickness and S-wave velocity profiles.

INTRODUCTION

Ambient vibration technique such as the H/V method and the more advanced array technique have the potential to significantly contribute to site characterization, and therefore to a more effective seismic risk mitigation, in particular in urban areas. In order to thoroughly test the actual capabilities of these H/V and array techniques under well-controlled conditions, within the framework of the SESAME project (Site EffectS Assessment using AMbient Excitations) we have simulated ambient seismic noise for a set of canonical models. The set of canonical models considered here is composed of 1D models (homogenous half-space, horizontally layered structure including model with velocity gradient) and 3D models (dipping layer and deep valley). The basic questions we want to address with these simulations are the following:

- 1) In horizontally stratified structures, are these techniques able to retrieve the right information on site characteristics (fundamental frequency, velocity profile) and/or its amplification characteristics (peak amplification, transfer function)?

¹ Laboratoire de Géophysique Interne et de Tectonophysique (LGIT), Université Joseph Fourier, Grenoble, France. sbonnefo@obs.ujf-grenoble.fr

² Swiss seismological Service, ETH Zurich, Switzerland. cornou@seismo.ifg.ethz.ch

³ Geophysical Institute, Slovak Academy of Sciences (GPI-SAS), Slovakia

⁴ Institute of Geosciences, University of Potsdam, Germany

⁵ Laboratoire Interdisciplinaire de Recherche Impliquant la Géologie et la Mécanique (LIRIGM), Université Joseph Fourier, Grenoble, France

- 2) In 2D or 3D structures, do these techniques based essentially on 1D surface wave interpretation provide relevant and useful results as to local site characteristics?

METHODS

Simulation of ambient noise

The numerical code that has been developed within the European SESAME project is intended to simulate ambient seismic noise originated by human activity, for sites with heterogeneous subsurface structures [1,2]. Noise sources are approximated by surface or subsurface forces, distributed randomly in space, direction (vertical or horizontal), amplitude, as well as in time. The time function is either delta-like signal (impulsive sources) or pseudo-monochromatic signal (“machine” sources) (a harmonic carrier with the Gaussian envelope). For 3D canonical models, computation of the associated wave field is performed using an explicit heterogeneous finite-difference scheme solving equations of motion in the heterogeneous visco-elastic medium with material discontinuities. For 1D canonical models, we have preferred to compute the Green functions of the medium using the wavenumber method developed by Hisada [3,4] on the basis of computation time considerations.

H/V ratio

The technique originally proposed by Nogoshi and Igarashi [5], and wide-spread after its promotion by Nakamura [6,7] aims at estimating some site characteristics related with the site transfer function, using microtremor measurements. It consists in deriving the ratio between the Fourier spectra of the horizontal and the vertical components of the microtremor recording obtained at the surface; this ratio is called thereafter the H/V ratio. While many scientists only trust the peak frequency of this ratio, interpreted as linked to the Rayleigh waves ellipticity and representative of the fundamental S-wave resonance frequency for sites with large enough impedance contrast, some other claim the H/V ratio provides a satisfactory estimate of the site S-wave transfer function.

In our study, the spectra of three components are calculated on the noise synthetics for 40 seconds long windows, these windows are overlapping by 20% of samples per windows. The resulting spectra are smoothed following Konno and Ohmachi [8], with a parameter b equal to 40. H/V ratio is calculated, for each window, dividing the quadratic mean of the horizontal spectra by the vertical spectrum. Then the final H/V ratio is obtained by averaging H/V from all windows.

Array analysis and inverted seismic profiles

The frequency-wavenumber based method (f - k) is one of the main array techniques used for deriving the phase velocity dispersion curves from ambient vibration array measurements. Although other techniques are available (SPAC for instance), in this study, we have used the high-resolution frequency-wavenumber analysis scheme proposed by Capon [9] on vertical component of noise synthetics. While the inversion of seismic velocity profiles were performed using a Neighbourhood algorithm developed within the SESAME project [10] after Sambridge [11].

CANONICAL MODELS

1D models

We consider here four 1D models representative of rock site (homogeneous half-space), or sediment sites: a first one with one single homogeneous layer, a second one with two homogeneous layers, and a third one with an inhomogeneous gradient layer over a half-space. Physical properties of these models are indicated in Table 1. The synthetics are computed for a total duration of 70 seconds, over a frequency range from 0.5 Hz to 8.5 Hz.

A) M1	H (m)	Vp (m/s)	Vs (m/s)	Rho (Kg/m ³)	Qp	Qs
Half-space	---	2000	1000	2.5	100	50
B) M2	H (m)	Vp (m/s)	Vs (m/s)	Rho (Kg/m ³)	Qp	Qs
Layer	25	1350	200	1.9	50	25
Half-space	---	2000	1000	2.5	100	50
C) M10	H (m)	Vp (m/s)	Vs (m/s)	Rho (Kg/m ³)	Qp	Qs
Layer 1	18	1350	250	1.9	50	25
Layer 2	18	1350	625	1.9	50	25
Half-space	---	2000	1500	2.5	100	50
D) M11	H (m)	Vp (m/s)	Vs (m/s)	Rho (Kg/m ³)	Qp	Qs
Layer	36	1350	200+5z	1.9	50	25
Half-space	---	2000	1000	2.5	100	50

Table 1: Physical model parameters considered for the 1D models a) half-space, b) one layer over a half-space, c) two layers over a half-space, c) a gradient layer over a half-space.

An array of 38 receivers having an aperture of 100 meters and a minimum sensor-to-sensor distance of 4 meters have been considered for the computation of noise synthetics (Figure 1). 333 sources located at 2 meters deep were placed around the array site within a radius of 300 meters (Figure 1).

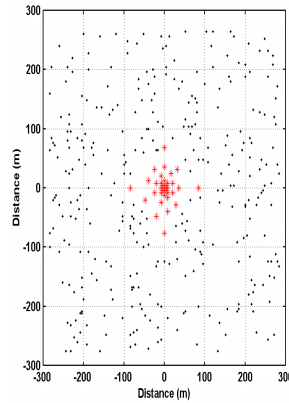
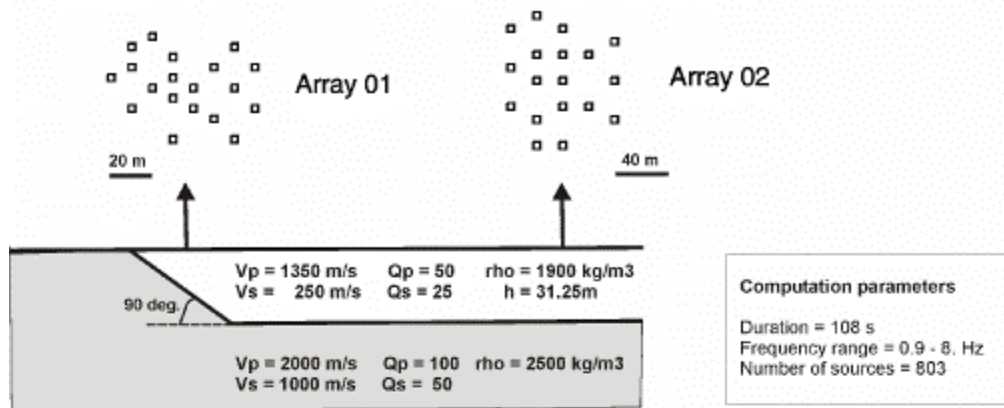


Figure 1: Configuration of the array composed of 38 receivers (red stars), the minimum distance between two receivers is 4 meters and the array aperture is 200 meters. 333 sources are located outside the array (black dots), there are located at 2 meters deep and their spatial extend is 600 meters.

3D models

We present here the simulations performed for two models: the first one (model M9A) corresponds to a valley edge and is characterized for a dipping layer overlaying a half-space, the second (model M7A) is a deep sedimentary valley with an elliptical shape. Their geometry and mechanical characteristics are indicated in Figure 2. In both cases we have considered in this study arrays located above the slope (arrays 01, Figure 2) and an array located above the flattest part of the model (array 02, Figure 2). For the arrays 01, the thickness of the sediments varies from 11 to 23 m and from 269 to 364 m throughout the array for models M9A and M7A, respectively. Sources were located at the free surface and receivers were located within the valley for the model M7A or throughout all the computation area for the model M9A.

Dipping layer over halfspace (model M9A)



Deep sediment valley (model M7A)

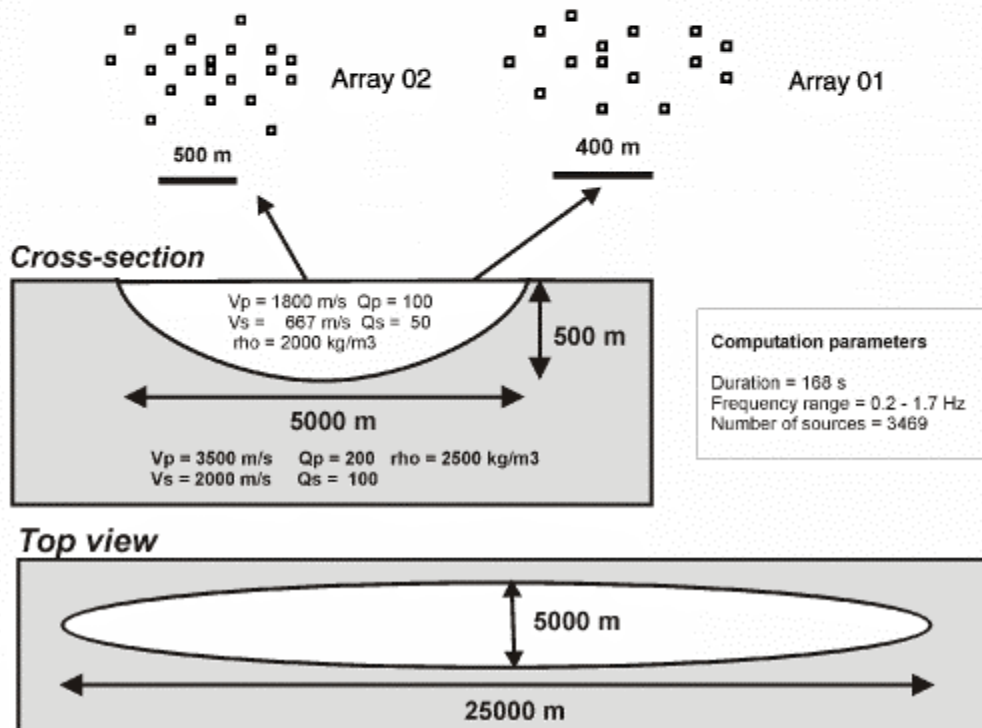


Figure 2: Models, array configuration and simulation parameters for 3D models, the M9A model (dipping layer over half-space) and the M7A model (deep sediment valley).

RESULTS

1D models

Rock site

The “synthetic” H/V ratio derived from the M1 model (half-space) is displayed in Figure 3 (left). As expected, the H/V curve is flat without any peak is exhibited. The dispersion curve derived from the array analysis (Figure 3, right) shows that non-dispersive waves having phase velocities close to the S-wave and Rayleigh wave velocities dominate the wave field in the M1 model.

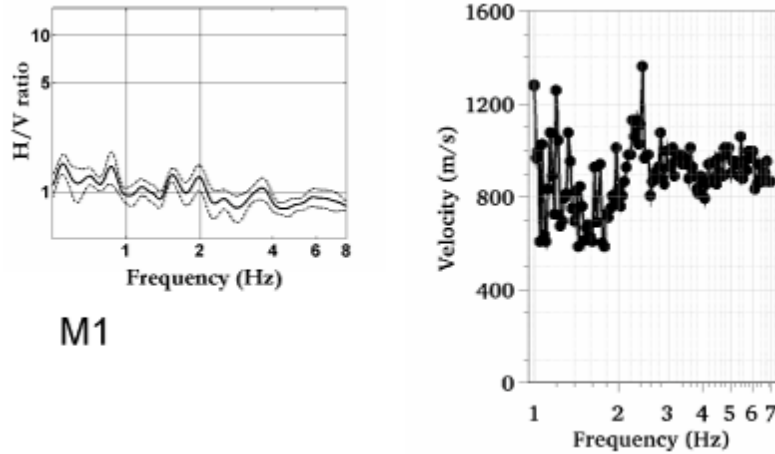


Figure 3: (Left) mean (black line) and standard deviation (black dashed line) of H/V ratio computed on all receivers from the half-space model. (Right) dispersion cure computed with CAPON analysis on vertical component.

H/V ratio

The H/V ratios observed on the M2, M10 and M11 models (respectively, the one layer, the two layers and the gradient layer overlying a half-space) exhibit one clear peak (Figure 4, left panel) having a frequency very close to the 1D resonance frequency given by the 1D transfer function computed for vertically incident S-wave. On contrary, the H/V ratio peak amplitude always over estimate the actual site amplification provided by the 1D transfer function for vertically incident plane S-wave (about 60% of overestimation). Then we can conclude that in case of 1D structure, the H/V ratio gives the resonant frequency of the structure, but over estimate the site amplification (at least on these three models).

Inverted S-wave velocity profiles

The inversion of S-wave velocity profiles has been performed using only a band-limited portion of the estimated dispersion curve: at low frequencies, the f-k analysis does not provide reliable results because of a) the limited array aperture and b) of the relatively small amount of energy emitted by the near surface sources considered in our noise generation model. The frequency range used for each of the three models is displayed on the right panel of Figure 4. For all the models, the S-wave velocities in the bedrock are not well constrained in the inversion (Figure 4, middle panel) since the S-wave velocities at frequencies below the resonance frequency of the site are indeed not correctly estimated by the array analysis. This is explained by the lack of coherent energy at frequencies below the resonance frequency of the site since we do not include in the simulation the effects of impinging coastal surface waves that propagate at low frequency throughout the crustal structure. For the M2 model (one layer over a half-space) and the M11 model (gradient layer), the inverted S-wave velocity profile is well estimated. For the M10 model (two layers over a half-space), although the S-wave velocity profile is well estimated for the superficial layer,

the S-wave velocity and the thickness of the second layer are not well constrained (we present here only the best S-wave velocity profiles obtained). This means that, in case of two layers with moderate contrast, we are not able to obtain the entire S-wave velocity profile by inversion, only the first layer parameters (S-wave velocity and thickness) are well defined.

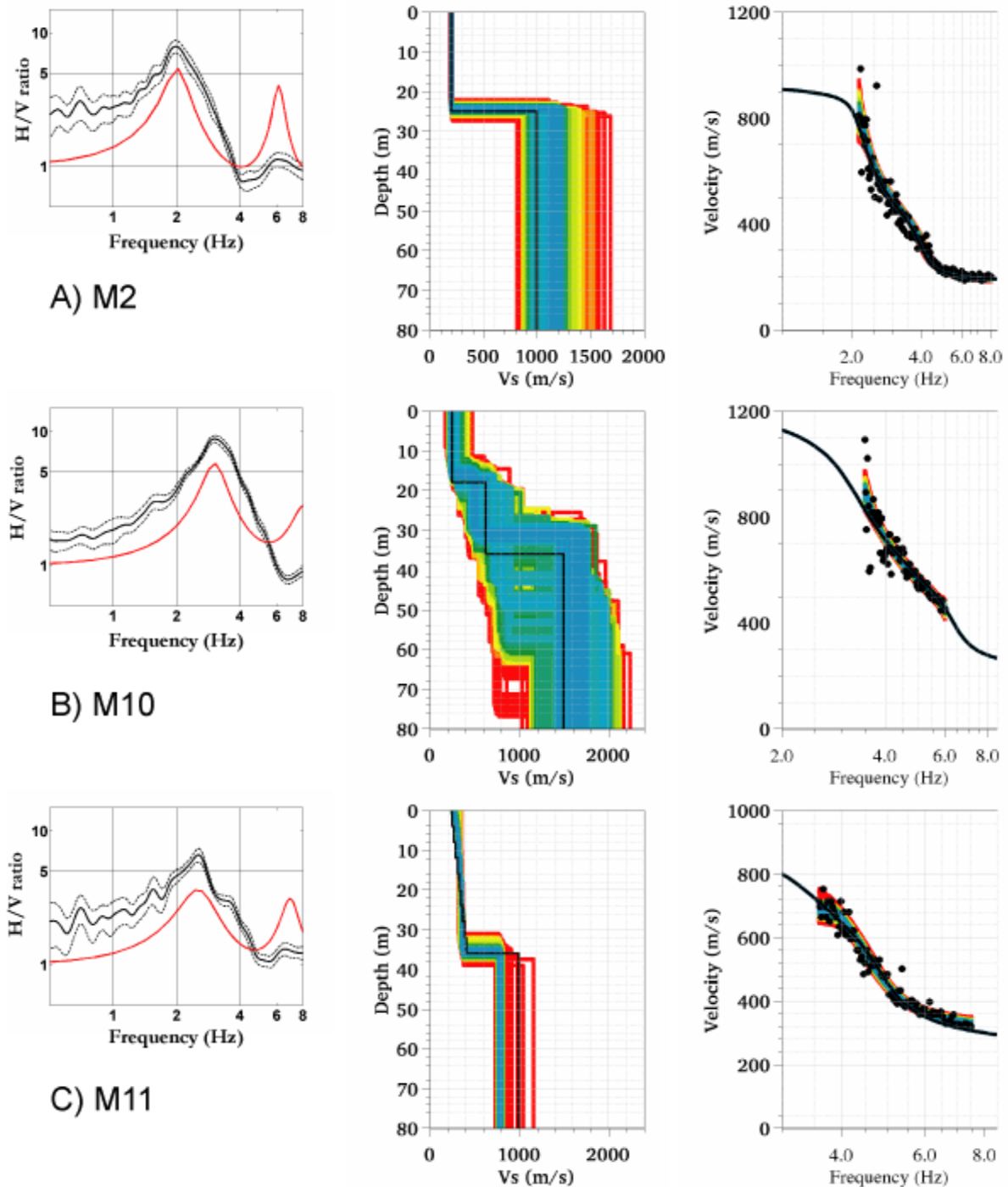


Figure 4: mean H/V ratio (left), inverted S-wave velocity profiles (middle) and dispersion curve (right) observed at the M2 model (A), the M10 model (B) and at the M11 model (C). Mean H/V ratios (thick line) and +/- standard deviation (thin lines) are computed on all receivers, the red line indicates the transfer function for vertically incident S-wave. The black line on the inverted S-wave velocity profile indicates the theoretical model. The best inverted seismic profiles are indicated by the blue color. The black dots on the

dispersion curve show the dispersion curve obtained from CAPON analysis on vertical component. The black line indicates the theoretical dispersion curve of the fundamental mode of Rayleigh waves.

3D models

Results of the H/V and the array analysis are presented in Figure 5 and Figure 6 for the M9A and M7A models, respectively.

H/V ratio

H/V curves are displayed in panels (B) and show, as expected, a decrease of the H/V peak frequency with an increase of the sediment thickness. For the flat portions of the M7A and M9A models, the H/V peak frequencies agree within a relative deviation of 15% with the 1D theoretical resonance frequency (Figures 5 and 6, C panels). On the contrary, H/V ratios obtained over the slopes exhibit two main features: on one hand, despite the impedance contrast is exactly the same as in the flat part of the model, the peak is both broader and much less pronounced so that picking a “peak frequency” is not an easy task; on the other hand, whenever it is possible to pick such a frequency, its value exhibit significant deviations from the theoretical 1D local value (the relative deviation ranges from 20 to 40% for both models). One can however detect a clear trend to increasing frequencies with decreasing local thickness.

Inverted S-wave velocity profiles

Inverted S-wave profiles and dispersion curves derived from array analysis are displayed in Figures 5 and 6 (panels A). For both models, the basement depth and the superficial S-wave velocity were fairly well estimated for arrays located above the flattest part of the sediments fill. For the deep sedimentary valley model (M7A), the inversion performed at the array located above the slope provides a bedrock depth at around 280 m that may be related to the average thickness of the sediments throughout the array. For the dipping layer model (M9A), the inversion has provided two classes of possible seismic profiles: the first class provides a bedrock depth at around 13 m and the other one a bedrock depth at around 30 m. This second class of solution comes from the fact that, since the noise is simulated up to 8 Hz, the array cannot correctly estimate the minimum phase velocity that occurs indeed at a higher frequency (considering a flat layer of 10 meters thickness the minimum phase velocity occurs at 16 Hz); and thus, the minimum S-wave velocity is not well constrained in the inversion. When constraining the minimum velocity to be around 250 m/s, the estimated bedrock depth is around 13 meters, a value which seems much more satisfactory, although is closer to the minimum sediment thickness throughout the array (11 meters) than to the average one (17 meters).

CONCLUSIONS

The aims of this study was 1) to investigate the abilities of the H/V and the array techniques to retrieve, for 1D structures, the right information on site characteristics (fundamental frequency and velocity profile); 2) to investigate the relevance of these techniques in case of 2D and 3D structures:

- 1) concerning the first point, the H/V shows is robustness to identify the resonance frequency for the 1D structures considered here (one layer, two layers, or a gradient layer overlaying a half-space). We show the same feature for the array analysis, this technique seems to be relevant to provide the S-wave velocity profile in case of 1D structure; though, in case of a moderate velocity contrast between two layers, array analysis techniques alone do have a sufficient resolution to clearly identify slight velocity changes with depth, and provide good estimates only of the wave velocity value for the superficial layer;

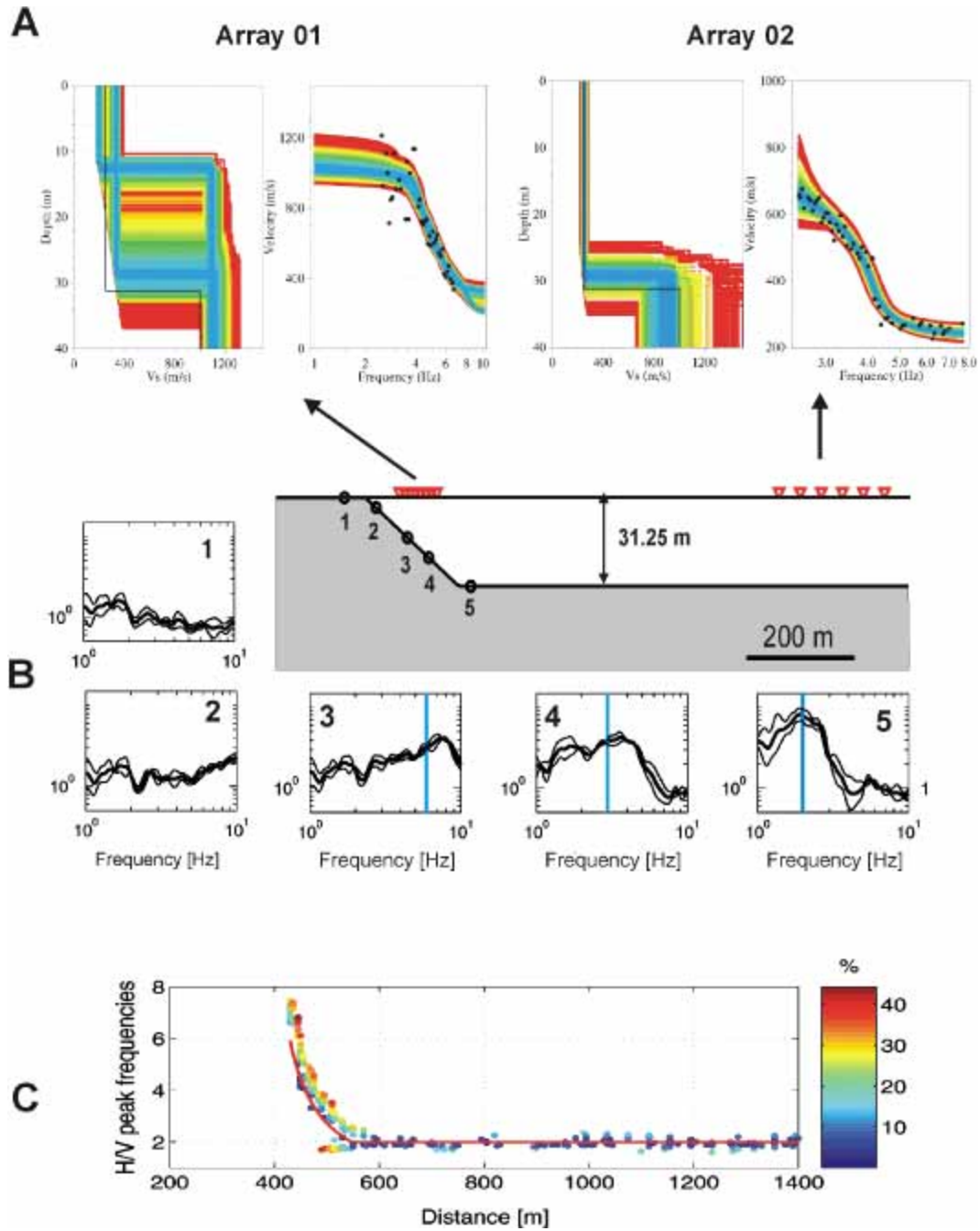


Figure 5: M9A model: (A) Inverted S-wave velocity profile (left) and dispersion curve (right). The best solutions are indicated by the blue color. (B) Model cross-section and H/V ratios (thick line) \pm standard deviation (thin lines) observed at different sites (1), (2), (3), (4), (5) along the cross-sections (the sites location are also indicated on the model cross section). The theoretical 1D local resonance frequency is indicated by a blue line. (C) H/V peak frequencies (points) estimated at all the receivers as function of the distance along the cross section displayed in (B). The 1D theoretical frequency is indicated by the red line. The color indicates the relative deviation in % of the H/V peak frequency from the 1D theoretical resonance frequency.

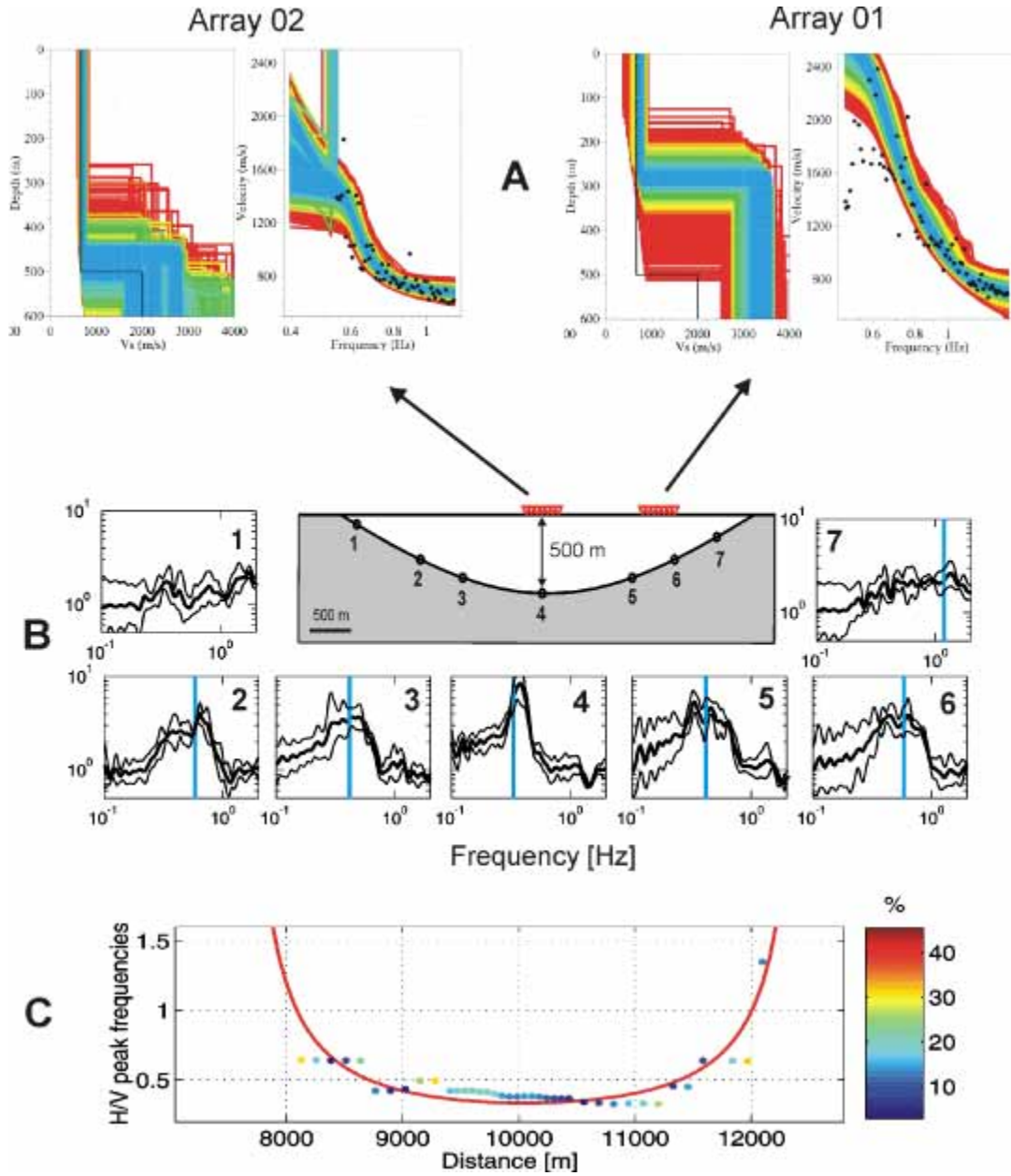


Figure 6: M7A model: (A) Inverted S-wave velocity profile (left) and dispersion curve (right). The best solutions are indicated by the blue color. (B) Model cross-section and H/V ratios (thick line) +/- standard deviation (thin lines) observed at different sites (1), (2), (3), (4), (5) along the cross-sections (the sites location are also indicated on the model cross section). The theoretical 1D local resonance frequency is indicated by a blue line. (C) H/V peak frequencies (points) as function of the distance along the cross section displayed in (B). The 1D theoretical frequency is indicated by the red line. The color indicates the relative deviation in % of the H/V peak frequency from the 1D theoretical resonance frequency. Only the receivers lying along the cross-section have been considered.

- 2) for the 3D structures considered here (dipping layer and deep sedimentary valley), the resonance frequency given by the H/V technique generally slightly overestimates the theoretical 1D resonance frequency (with a deviation range of about 20%). The pH/V peaks, however, are much less clear on sites with rapidly varying thickness. The S-wave velocity profile inverted from arrays located over underground slopes is basically related with the average thickness and S-wave velocity of the structure under the array; in the areas where the underground structure does not present rapid lateral variations, the inverted velocity profiles are as satisfactory as in fully 1D structures.

Although this study does point out some limitations for the array analysis techniques, their ability to give the superficial S-wave velocity is highlighted. A way to obtain the entire S-wave velocity profile of a complex structure could be to couple geophysical methods such as seismic refraction. In fact, in many cases, the seismic refraction method is able to give the thickness of layers, so it could be interesting to constrain the depth of the bedrock and then obtain the superficial S-wave velocity with array analysis.

ACKNOWLEDGEMENTS

The SESAME project (Project No. EVG1-CT-2000-00026) is supported by the European Commission – Research General Directorate.

REFERENCES

1. Moczo P, Kristek J, Vavrycuk V, Archutela R, Halada L. “3D heterogeneous staggered-grid finite-difference modeling of seismic motion with volume harmonic and arithmetic averaging of elastic moduli and densities.” *Bulletin of the Seismological Society of America* 2002; 92(8): 3042-3066.
2. Moczo P, Kristek J. “FD code to generate noise synthetics.” Final report, project No EVG1-CT-2000-00026 SESAME 2002; 31 pp.
3. Hisada Y. “An efficient method for computing Green’s functions for a layered half-space with sources and receivers at close depths.” *Bulletin of the Seismological Society of America* 1994; 84(5): 1456-72.
4. Hisada Y. “An efficient method for computing Green’s functions for a layered half-space with sources and receivers at close depths (part 2).” *Bulletin of the Seismological Society of America* 1995; 85(4): 1080-93.
5. Nogoshi M, Igarashi T. “On the amplitude characteristics of microtremor (part 2) (in Japanese with English abstract).” *Journal of Seismological Society of Japan* 1971; 24: 26-40.
6. Nakamura Y. “A method for dynamic characteristics estimation of subsurface using microtremor on the ground surface.” *Quarterly Report Railway Tech. Res. Inst.* 1989; 30(1): 25-30.
7. Nakamura Y. “Real-time information systems for hazards mitigation.” *Proceedings of the 11th World Conference on Earthquake Engineering*, Acapulco, Mexico. Paper no. 2134, 1989.
8. Konno K, Ohmachi T. “Ground-motion characteristics estimated from spectral ratio between horizontal and vertical components of microtremor.” *Bulletin of the Seismological Society of America* 1998; 88(1): 228-41.
9. Capon J. “High-resolution frequency-wavenumber spectrum analysis.” *Proceedings of the I.E.E.*, 1969.
10. Wathelet M, Jongmans D, Ohrnberger M. “Surface wave inversion using a direct search algorithm and its application to ambient vibrations measurements.” *Near Surface Geophysics* (In press).
11. Sambridge M. “Geophysical inversion with a neighbourhood algorithm I. Searching a parameter space.” *Journal of Geophysical Research* 1999; 103: 4839-78.